



# Prussian blue-derived $\text{Fe}_2\text{O}_3$ /sulfur composite cathode for lithium–sulfur batteries

Chongchong Zhao<sup>a,b</sup>, Cai Shen<sup>a,1</sup>, Fengxia Xin<sup>a</sup>, Zixu Sun<sup>a</sup>, Weiqiang Han<sup>a,1</sup>

<sup>a</sup> Ningbo Institute of Materials Technology & Engineering, Chinese Academy of Sciences, 1219 Zhongguan Road, Zhenhai District, Ningbo, Zhejiang, China

<sup>b</sup> Faculty of Materials, Optoelectronics and Physics, Xiangtan University, Xiangtan, China

## ARTICLE INFO

### Article history:

Received 19 July 2014

Accepted 20 August 2014

### Keywords:

Nanoparticles

Energy storage and conversion

## ABSTRACT

Porous  $\text{Fe}_2\text{O}_3$  was prepared by simple annealing of preformed Prussian blue that was synthesized from a wet chemistry method. The obtained porous  $\text{Fe}_2\text{O}_3$  nanoparticles were then mixed with sulfur and used as cathode for lithium–sulfur batteries. The porous  $\text{Fe}_2\text{O}_3$  acts as an internal polysulfide reservoir, and thus reduces the shuttle effect. Composite cathode containing 5% porous  $\text{Fe}_2\text{O}_3$  shows improved cycling performance as compared to that without porous  $\text{Fe}_2\text{O}_3$ . A stable reversible discharge capacity of 574.3 mAh/g was obtained after 50 cycles at 0.5 C.

© 2014 Published by Elsevier B.V.

## 1. Introduction

Lithium–sulfur (Li/S) battery is a promising electrochemical system with possibility of achieving high-energy up to a theoretical capacity of 1675 mAh/g [1–4]. Combined with other advantages of sulfur such as low toxicity and natural abundance, it has attracted wide attention especially for applications of next generation energy storage and hybrid vehicles. However, the system suffers from several drawbacks particularly dissolution of intermediate polysulfide reaction species into electrolyte [5–10]. Thus, novel advances in materials design such as new electrolytes [11–20], polymer coated sulfur nanosphere core/cell structure and conductive mesoporous/nano carbon framework for constraining sulfur have been proposed [21–35]. These techniques significantly improve the cycling performance of Li/S batteries but falls short of completely controlling polysulfide dissolution. Recently, a new concept of embedding small fraction of porous silica particles (SBA-15) within carbon–sulfur nanocomposites which act as an internal polysulfide reservoir has been proposed by Nazar et al. to stabilize the system [36]. The results show greatly improved cycling stability and less polysulfide shuttle effect. In line with this concept, here we report the synthesis of porous  $\text{Fe}_2\text{O}_3$  and the use of it as polysulfide reservoir in sulfur cathode to improve the performance of Li/S batteries. A doping of 5% porous  $\text{Fe}_2\text{O}_3$  shows improved cycling performance with more stable reversible discharge capacity of ca. 574 mAh/g after 50 cycles.

## 2. Materials and methods

**Synthesis and characterization of porous  $\text{Fe}_2\text{O}_3$ :** Porous microcubes  $\text{Fe}_2\text{O}_3$  was prepared from annealing of preformed Prussian blue synthesized from precursors of Polyvinylpyrrolidone (PVP), potassium ferrocyanide ( $\text{K}_4\text{Fe}(\text{CN})_6 \cdot 3\text{H}_2\text{O}$ ) and HCl solution. Firstly, Polyvinylpyrrolidone (PVP, 15.2 g) and potassium ferrocyanide ( $\text{K}_4\text{Fe}(\text{CN})_6 \cdot 3\text{H}_2\text{O}$ , 0.44 g) were added to a HCl solution (0.1 M, 200 ml) under magnetic stirring to obtain a clear solution which was heated at 80 °C for 12 h. The solution was then washed several times with distilled water and ethanol solution and then centrifuged. The sediment was dried in a vacuum oven at 30 °C for 10 h. Finally, this product was heated at 500 °C for 5 h in air with a temperature ramp of 2 °C/min and naturally cooled to room temperature to obtain a porous micro boxes  $\text{Fe}_2\text{O}_3$ . The products were measured by X-ray diffraction (XRD, D8 Discover, Broker AXS), scanning electron microscopy (SEM, S-4800, Hitachi), transmission electron microscope (TEM, Tecnai F20, FEI) and thermogravimetric analysis (Pyris Diamond TG, Perkin-Elmer).

**Electrode fabrication and electrochemical measurement:** The electrochemical measurements were carried out using 2032-type coin cell system. S/ $\text{Fe}_2\text{O}_3$  composite was prepared by simple mixing S and porous  $\text{Fe}_2\text{O}_3$  particles at room temperature. Cathode electrodes were prepared by coating a mixture containing 70 wt% S/ $\text{Fe}_2\text{O}_3$  (1%  $\text{Fe}_2\text{O}_3$  doping=69.3 wt% sulfur loading, 5%  $\text{Fe}_2\text{O}_3$  doping=66.5 wt% sulfur loading, 10%  $\text{Fe}_2\text{O}_3$  doping=63 wt% sulfur loading) composite, 20 wt% conductive carbon black (super P), and 10 wt% polyvinylidene fluoride (PVDF) dissolved in N-methyl-2-pyrrolidone (NMP) to form a slurry onto Cu current collector. The test electrodes were dried at 50 °C in a vacuum for 20 h, the electrode film was cut into sheets of 14 mm in diameter, pressed and dried for another 2 h at 50 °C, and the composite loading is

E-mail addresses: [shencai@nimte.ac.cn](mailto:shencai@nimte.ac.cn) (C. Shen), [hanweiqiang@nimte.ac.cn](mailto:hanweiqiang@nimte.ac.cn) (W. Han).  
<sup>1</sup> Tel.: +86 574 86685146; fax: +86 574 87910728.

<http://dx.doi.org/10.1016/j.matlet.2014.08.115>  
 0167-577X/© 2014 Published by Elsevier B.V.

about 1.2 mg/cm<sup>2</sup>. Then 2032-type coin cells were fabricated for electrochemical testing in an argon-filled glovebox which oxygen and moisture concentrations below 0.1 ppm. Metallic lithium was used as the counter/reference electrode, 1 M lithium bis(trifluoromethane sulfonimide)imide (LiTFSI) in dioxolane/dimethoxyethane solvent (DOL/DME, volume ratio=1:1) was used as electrolyte, and Celgard 2400 polypropylene as separator. Charge/discharge measurements were carried out galvanostatically at various current densities (1 C=1675 mAh/g) over a voltage range of 1.0–3.0 V(vs. Li/Li<sup>+</sup>) using a battery test system(LAND model, CT2001A, Wuhan RAMBO testing equipment, Co. Ltd.) at 30 °C.

### 3. Results and discussion

Fig. 1(a) shows the SEM image of as-synthesized Prussian blue microcubes. Those microcubes are quite uniform with an average size of ca. 300 nm due to the face-centered-cubic (fcc) crystal structure of Fe<sub>4</sub>[Fe(CN)<sub>6</sub>]<sub>3</sub>. These as-synthesized Prussian blue microcubes were transformed into porous Fe<sub>2</sub>O<sub>3</sub> microcubes by annealing in air. As indicated by the thermogravimetric analysis (TGA) shown in Fig. 1(b), the Prussian blue microcubes underwent

significant weight loss during heating. A loss of ~40% of weight was found under 320 °C, which is mainly due to the thermally induced oxidative decomposition. The decomposition process is accompanied by outward gas flow, which eventually resulted in formation of cavities.

From SEM image and TEM image shown in Fig. 1(c) and (d), it was found that highly porous cubic structures were obtained at 500 °C. These porous microcubes were consisted of Fe<sub>2</sub>O<sub>3</sub> nanoparticles with sizes of tens of nanometers and cavities with size in the range of 1–10 nm. At lower temperature, no porous structures were observed, while higher temperature heating resulted in the continued growth of Fe<sub>2</sub>O<sub>3</sub> pore size and the aggregation of Fe<sub>2</sub>O<sub>3</sub> nanoparticles.

The crystallographic structure of the porous structures annealed at 500 °C was further examined by powder X-ray diffraction (XRD). As shown in Fig. S1, although there are a few small peaks which are difficult to be assigned possibly due to incomplete oxidation of Fe<sub>2</sub>O<sub>3</sub>, most of the main diffraction peaks could be assigned to Fe<sub>2</sub>O<sub>3</sub> as indicated in the figure.

To study the effects of porous Fe<sub>2</sub>O<sub>3</sub> incorporation on electrochemical performance in Li-S batteries, sulfur and Fe<sub>2</sub>O<sub>3</sub>/S composite electrodes were prepared (see the experimental method). Fig. 2 shows the SEM images of sulfur cathode without Fe<sub>2</sub>O<sub>3</sub>

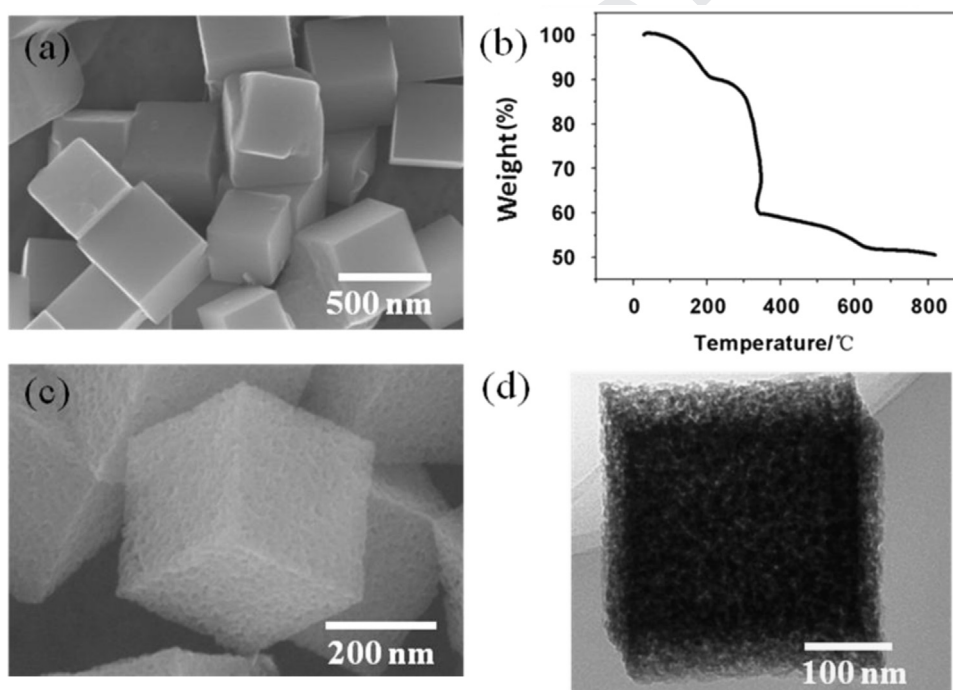


Fig. 1. (a) SEM image of as-prepared Prussian blue microcubes, (b) TGA of the as-prepared Prussian blue microcubes in air, (c) SEM image of Prussian blue microcubes annealed at 500 °C, and (d) TEM image of Prussian blue microcubes annealed at 500 °C.

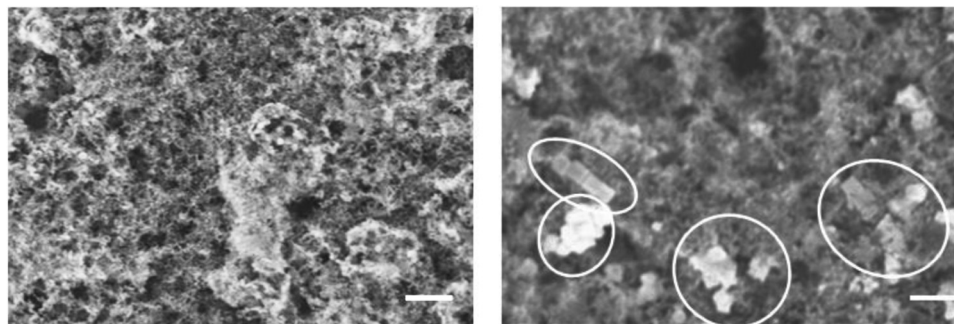
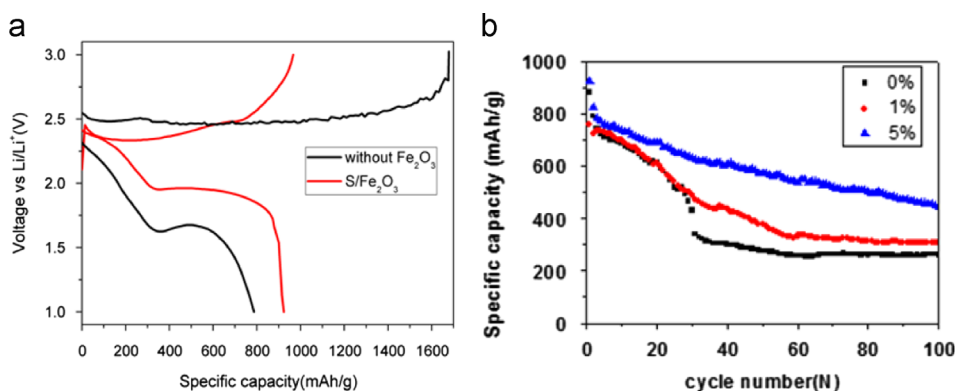


Fig. 2. SEM images of sulfur cathode without Fe<sub>2</sub>O<sub>3</sub> (a), and composite electrodes with 5% Fe<sub>2</sub>O<sub>3</sub> nanoparticles. Scale bar: 1 μm.



**Fig. 3.** Electrochemical data for  $\text{Fe}_2\text{O}_3/\text{S}$  composite electrode as compared to the sulfur electrode. Data were obtained on galvanostatic cycling at a C/2 rate (corresponds to a current density of 837.5 mA/g) and voltage window of 1.0–3.0 V. (a) Comparison of the charge–discharge profiles of the first cycle of  $\text{Fe}_2\text{O}_3$  (5%, weight)/S composite electrode and pure S electrode system. (b) Electrochemical data for various  $\text{Fe}_2\text{O}_3/\text{S}$  composite electrodes compared with the sulfur electrode.

doping and with  $\text{Fe}_2\text{O}_3$  doping. From Fig. 2b, it is clearly found that the cubic structure of porous of  $\text{Fe}_2\text{O}_3$  (indicated in the white boxes as shown in Fig. 2b) is well-maintained after mixing with sulfur.

Electrochemical measurements of the assembled coin cells were then carried out in the voltage range of 1.0–3.0 V. As shown in Fig. 3(a), a discharge specific capacity of 787.2 mAh/g at a rate of 0.5 C was observed in the pure sulfur system. Meanwhile, the 5%  $\text{Fe}_2\text{O}_3/\text{S}$  composite electrode shows a higher specific capacity of 923.5 mAh/g under similar condition. The increment of the first discharge capacity from  $\text{Fe}_2\text{O}_3/\text{S}$  electrode could be due to contribution of the discharge capacity of  $\text{Fe}_2\text{O}_3$ . It was also found that both cells with or without porous  $\text{Fe}_2\text{O}_3$  incorporation exhibited irreversible capacity in the first cycle. However, such effect is much lesser in cell with porous  $\text{Fe}_2\text{O}_3$  incorporation (95.6% for  $\text{Fe}_2\text{O}_3/\text{S}$  vs. 46.9% for S electrode). This implies polysulphide shuttle mechanism is significantly mitigated due to the incorporation of porous  $\text{Fe}_2\text{O}_3$ , which acts as an internal polysulfide reservoir to reduce the shuttle effect.

The 5%  $\text{Fe}_2\text{O}_3/\text{S}$  composite system not only improved the first discharge capacity, but also shows an improved cycling stability as shown in Fig. 3(b). A reversible capacity of 574.3 mAh/g and 442.3 mAh/g were obtained after 50 cycles and 100 cycles, respectively. Other ratios of  $\text{Fe}_2\text{O}_3/\text{sulfur}$  composite electrodes were also tested. It was found that both the lower  $\text{Fe}_2\text{O}_3$  doping (1% weight) and higher  $\text{Fe}_2\text{O}_3$  doping (5% weight)  $\text{Fe}_2\text{O}_3/\text{S}$  composite systems have improved cycling stability (Fig. 3b), however, doping of over 10% of  $\text{Fe}_2\text{O}_3$  resulted in low performance of batteries due to insufficient loading of the active element of sulfur. One should note that although  $\text{Fe}_2\text{O}_3$  has long been reported as an anode material for lithium ion batteries, the use of  $\text{Fe}_2\text{O}_3$  as cathode do not contribute significant capacity (only 50 mAh/g at 1 C) under the measured voltage range (1–3 V).

We noticed that in all cases of different amount of  $\text{Fe}_2\text{O}_3$  doping, the shuttle effect still exists. This kind of composite electrodes seem unable to completely eliminate the polysulfide dissolution probably due to inhomogeneous of the  $\text{Fe}_2\text{O}_3$  pore sizes. Further study on the effects of pore sizes on Li–S system is on the way to elucidate the shuttle effect. Stable metal–organic framework with tunable pore size could be a better candidate as polysulfide reservoir.

#### 4. Conclusion

In summary, porous  $\text{Fe}_2\text{O}_3$  with size of  $\sim 300$  nm and cavities in the range of 1–10 nm was prepared from simple annealing of preformed Prussian blue. For the first time, we observed that

porous  $\text{Fe}_2\text{O}_3$  incorporation stabilized the cycling with a higher specific capacity than the pure sulfur cathode Li–S battery system. Our strategy based on the facile doping of porous structure rather than synthesis of complex S/C or other core/shell structures provides a new route for stabilizing the Li–S system and could be more practical for mass application with low cost and good repeatability.

#### Acknowledgments

We thank the National Natural Science Foundation of China (Grant nos. 51371186 and 21303236), the recruitment program of global experts of Central Organization Department, the Ningbo “3315 group plan”, and the NIMTE (Y20838RA23, Y30805WA06 and Y30806RA05). Cai thanks the financial support from Ningbo “3315 individual plan” and SRF for ROCS, SEM.

#### Appendix A. Supporting information

Supplementary data associated with this article can be found in the online version at <http://dx.doi.org/10.1016/j.matlet.2014.08.115>.

#### References

- [1] Bruce PG, Freunberger SA, Hardwick LJ, Tarascon JM. *Nat Mater* 2012;11:19.
- [2] Barghamadi M, Kapoor A, Wen C. *J Electrochem Soc* 2013;160:A1256.
- [3] Ji X, Nazar LF. *J Mater Chem* 2010;20:9821.
- [4] Su Y, Manthiram A. *Nat Commun* 2009;8:500.
- [5] Song MK, Cairns EJ, Zhang Y. *Nanoscale* 2013;5:2186.
- [6] Diao Y, Xie K, Xiong S, Hong X. *J Electrochem Soc* 2012;159:A421.
- [7] Diao Y, Xie K, Xiong S, Hong X. *J Power Sources* 2013;235:181.
- [8] Mikhaylik YV, Akridge JR. *J Electrochem Soc* 2004;151:A1969.
- [9] Cheon S-E, Choi S-S, Han J-S, Choi Y-S, Jung B-H, Lim HS. *J Electrochem Soc* 2004;151:A2067.
- [10] Choi NS, Chen Z, Freunberger SA, Ji X, Sun YK, Amine K, et al. *Angew Chem Int Ed Engl* 2012;51:9994.
- [11] Yang Y, Zheng G, Cui Y. *Energy Environ Sci* 2013;6:1552.
- [12] Suo L, Hu YS, Li H, Armand M, Chen L. *Nat Commun* 2013;4:1481.
- [13] Zhang SS, Read JA. *J Power Sources* 2012;200:77.
- [14] Zhang SS. *J Power Sources* 2013;231:153.
- [15] Ryu H-S, Ahn H-J, Kim K-W, Ahn J-H, Cho K-K, Nam T-H, et al. *J Power Sources* 2006;163:201.
- [16] Wang J, Chew SY, Zhao ZW, Ashraf S, Wexler D, Chen J, et al. *Carbon* 2008;46:229.
- [17] Zheng J, Gu M, Chen H, Meduri P, Engelhard MH, Zhang J-G, et al. *J Mater Chem A* 2013;1:8464.
- [18] Wang JL, Yang J, Xie JY, Xu NX, Li Y. *Electrochem Commun* 2002;4:499.
- [19] Kim HS, Jeong T-G, Choi N-S, Kim Y-T. *Ionics* 2013;19:1795.
- [20] Barchasz C, Lepretre JC, Patoux S, Allouin F. *J Electrochem Soc* 2013;160:A430.
- [21] Wei Seh Z, Li W, Cha JJ, Zheng G, Yang Y, McDowell MT, et al. *Nat Commun* 2013;4:1331.
- [22] Ji X, Evers S, Black R, Nazar LF. *Nat Commun* 2011;2:325.

- [23] Yang Y, Yu G, Cha JJ, Wu H, Vosgueritchian M, Yao Y, et al. ACS Nano 2011;5:9187.
- [24] Chen R, Zhao T, Lu J, Wu F, Li L, Chen J, et al. Nano Lett 2013;13:4642.
- [25] Wang J, Yin L, Jia H, Yu H, He Y, Yang J, et al. ChemSusChem 2014;7:563.
- [26] Shao J, Li X, Zhang L, Qu Q, Zheng H. Nanoscale 2013;5:1460.
- [27] Chen H, Dong W, Ge J, Wang C, Wu X, Lu W, et al. Sci Rep 2013;3:1910.
- [28] Zhou X, Xie J, Yang J, Zou Y, Tang J, Wang S, et al. J Power Sources 2013;243:993.
- [29] Marmorstein D, Yu TH, Striebel KA, McLarnon FR, Hou J, Cairns EJ. J Power Sources 2000;89:219.
- [30] Jeong S, Bresser D, Buchholz D, Winter M, Passerini S. J Power Sources 2013;235:220.
- [31] Zheng G, Zhang Q, Cha JJ, Yang Y, Li W, Seh ZW, et al. Nano Lett 2013;13:1265.
- [32] Cheng X-B, Huang J-Q, Peng H-J, Nie J-Q, Liu X-Y, Zhang Q, et al. J Power Sources 2014;253:263.
- [33] Chen S, Dai F, Gordin ML, Wang D. RSC Adv 2013;3:3540.
- [34] Yang Y, Zheng G, Cui Y. Chem Soc Rev 2013;42:3018.
- [35] Ding B, Yuan C, Shen L, Xu G, Nie P, Zhang X. Chemistry 2013;19:1013.
- [36] Ji X, Lee KT, Nazar LF. Nat Mater 2009;8:500.

10  
11  
12  
13  
14  
15  
16  
17